COMPUTATIONAL ACOUSTICS - Volume 2
D. Lee, A. Cakmak, R. Vichnevetsky (Editors)
Elsevier Science Publishers B.V. (North-Holland)

Perturbation Methods for Rays and Beams

Robert L. Nowack
Department of Earth and Atmospheric Sciences
Purdue University
West Lafayette, IN 47907

Abstract

Perturbation methods for rays and beams for small changes in medium parameters are discussed in this paper. These techniques are applicable to seismic modeling where a simpler nearby medium can be used to approximately calculate wavefields in more complicated media. This can also be used to compute wavefields in slightly anisotropic media, where calculations can be done in a nearby isotropic structure. For S-wave anisotropy and shear wave splitting, degenerate perturbation theory must be used. An extension to perturbed Gaussian beams is given where Gaussian beam seismograms are more complete near caustics and other critical regions. Also, since Gaussian beam seismograms don't require two-point ray tracing, this requires one less approximation for the perturbation analysis. Finally, perturbation methods can be used to compute functional derivatives and sensitivity operators for seismic inversion.

1. Introduction

In this paper, perturbation methods for rays and beams in heterogeneous media are discussed. Perturbation methods are applied to both isotropic and anisotropic media. An important application of perturbation theory is to seismic modeling where simpler models can be used to approximately compute wavefields in more complicated media. This type of analysis is also useful in checking more complete seismic synthesis techniques. Further investigations are needed in order to construct higher order perturbation formulations as well as to quantify regions of validity for the perturbation analysis.

For anisotropic media, perturbation methods are discussed which use ray calculations in a nearby isotropic medium (see also Nowack and Pšenčík, 1988). For shear waves, degenerate perturbation theory is required. The calculation of perturbed amplitudes in anisotropic media still involves extensive developmental work.

An extension to perturbed Gaussian beam seismograms is implemented. Gaussian beam theory gives more complete results at caustics and other singular regions than ray methods. Gaussian beams have the additional advantage of not using two-point ray tracing. For perturbed Gaussian beams, this requires one less approximation in the perturbation analysis.

A final application of seismic perturbation theory is to seismic inversion. Perturbation theory can be used to construct functional derivatives which are required for linear inversion. Preliminary test inversions using ray amplitude and travel-time have been conducted for velocity and interface parameters by Nowack and Lyslo (1988). However, further work is required to quantify the accuracy of the resulting functional derivatives as applied to seismic inversion.

2. Perturbation Methods in Isotropic Media

Seismic calculations in perturbed isotropic media are important in both forward modeling and seismic inversion. In the first part of this paper, perturbation theory for travel-times and ray theoretical amplitudes in heterogeneous media with curved interfaces is investigated.

The travel-time along a ray can be written

$$T = \int_{s_0}^{s} L(u(\underline{x}), \underline{x}, \dot{\underline{x}})\, ds \tag{2.1}$$

where $L = u(\underline{x})(\dot{x}_i \dot{x}_i)^{\frac{1}{2}}$ and $u(\underline{x})$ is the slowness. The first variation of the travel-time can be written

$$\delta T \approx \frac{\partial L}{\partial \dot{x}_i}\, \delta x_i \,|_{s_0}^{s} + \int_{s_0}^{s} \left\{ \frac{\partial L}{\partial x_i} - \frac{d}{ds} \frac{\partial L}{\partial \dot{x}_i} \right\} \delta x_i \, ds + \int_{s_0}^{s} \delta u(\underline{x})\, ds \tag{2.2}$$

Assuming no slowness perturbations and fixed end points, then for a geometric ray, $\delta T = 0$. Using Eq. (2.2), this results in the isotropic ray equations, $\frac{\partial L}{\partial x_i} - \frac{d}{ds}\left[\frac{\partial L}{\partial \dot{x}_i}\right] = 0$.

For a geometric ray with fixed endpoints, the perturbation of the travel-time due to a variation in the material slowness, $u(x)$, is given by the third term in Eq. (2.2). Thus, $\delta T \approx \int_{s_0}^{s} \delta u(\underline{x})\, ds$, where to first order this is computed along the original unperturbed ray path. Using the unperturbed ray path for the calculation of the travel-time perturbation is a major simplification which is utilized in most travel-time tomography algorithms (see, for example, Aki et. al., 1977).

For a geometric ray which is reflected or transmited from a curved boundary, then the first term in Eq. (2.2) is nonzero and can be written

$$\delta T \approx \frac{\partial L}{\partial \dot{x}_i}\, \delta x_i \int_{s_a^+}^{s_a^-} = p_i\, \delta x_i \,|_{s_a^+}^{s_a^-}$$

where s_a^- is for the incident ray and s_a^+ is for the reflected/transmitted ray. If the boundary shape is perturbed from $\sum_0$ to $\sum_p$, then the perturbation in the travel-time can be written

$$\delta T \approx \left\{ p_h^- - p_h^+ \right\} \delta h$$

where p_h is the normal component of the slowness vector and δh is the normal component of the boundary perturbation at the point of incidence. This is a first order approximation only since it assumes slowly varying material slowness or velocity near the boundary. A more complete formulation includes the effects of velocity near the boundary (see Farra et.al, 1988).

The above formula can be related to a node perturbation of an interpolated boundary, where a splined boundary is assumed. The spline coefficients for a perturbation of an interface node are

computed and from this the values of $\frac{\partial h(x_a)}{\partial z(x_{node})}$ can be found. The first variation of travel-time with respect to a perturbation of a boundary node of an interace can then be written

$$\delta T \approx \frac{\delta T}{\delta h(z_a)} \frac{\delta h(z_a)}{\partial z(x_{node})} \delta z(x_{node})$$

For the special case of a piecewise linear boundary and an incident reflected ray, this reduces to the results given by Bishop et al. (1985).

In the ray theoretical approximation, the seismic amplitude of a multiple reflected and transmitted ray can be written (see Červený, 1985a)

$$\hat{U}(O_s) = A(O_s)\, \hat{C}(O_s) \prod_{i=1}^{1} [\hat{R}(O_i)\, \hat{G}^L(O_i)]\, \hat{\Psi} \tag{2.3}$$

where $\hat{C}$ is the complete receiver matrix, $\hat{R}$ is the reflection/transmission matrix, $\hat{\Psi}$ is the source matrix, and $\hat{G}^L$ is the rotation matrix at each interface. $A(O_s)$ can be written

$$A(O_s) = \frac{1}{[v(O_s)\, \rho(O_s)\, \det Q(O_s)]^{\frac{1}{2}}} \prod_{i=1}^{N} [\frac{v'(O_i)\, \rho'(O_i)\, \det Q'(O_i)}{v(O_i)\, \rho(O_i)\, \det Q(O_i)}]^{\frac{1}{2}} \tag{2.4}$$

where O_s is the at the receiver and O_i is the i^{th} reflection/transmission point. $v(O_i)$ is the velocity and $\rho(O_i)$ is the density. The unprimed values are on the incident ray side of the boundary and the primed values are on the reflected/transmitted side. $Q(O_s)$ is a 2 x 2 matrix derived from

$$X(O_s) = \begin{bmatrix} Q(O_s) \\ \\ P(O_s) \end{bmatrix} = \pi(O_s, O_N) \prod_{i=N}^{1} [F(O_i)\pi(O_i, O_{i-1})]\; X(O_0)$$

where $\pi(O_i, O_{i-1})$ are the component ray propagator solutions to the dynamic ray equations for each layer with $\pi(O_i, O_i) = I$ (see Červený, 1985a). $F(O_i)$ is the transformation matrix at each interface. With appropriate initial conditions, $\det Q(O_s)$ is the geometric spreading.

The problem is now to find the approximate amplitude perturbation, $\delta\hat{U}(O_s)$, for a perturbation of either a smooth velocity or an interface node. The resulting perturbation of the ray amplitude is made up of two parts, the variation of the amplitude along the original ray path and the variation due to the shift of the ray. Farra and Madarriaga (1987) and Nowack and Lutter (1988) give results for the perturbation in the geometric spreading part of the amplitude from a smooth variation in velocity or slowness. Nowack and Lyslo (1988) give a strategy for the perturbation of the complete ray amplitude of a reflected/transmitted ray.

The first step in the amplitude perturbation for a direct ray is the calculation of the ray shift due to a smooth material slowness perturbation. The change in the transverse ray position, δp_r, in ray centered coordinates can be derived using the dynamic ray equations by introducing an effective

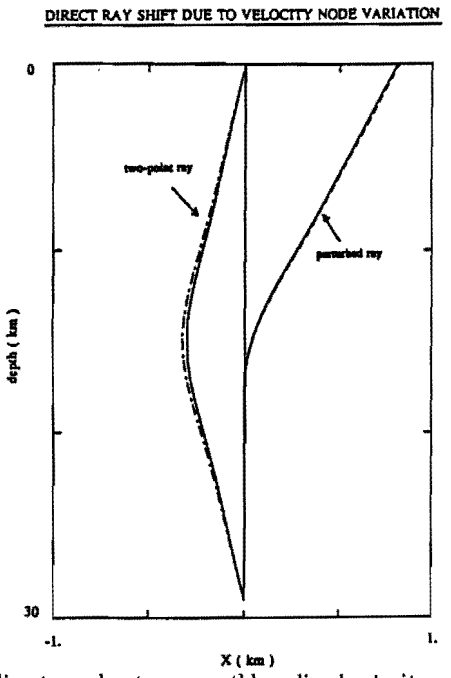

Figure 1: Ray shift for a direct ray due to a smoothly splined velocity node perturbation at (-2.,15.) increased in velocity by 2% above the background.

source term (see Farra and Madariaga, 1987, and Nowack and Lutter 1988). The solution for the ray shift can be written in terms of an integration of the ray propagator, $\pi_0(s, s')$, of the unperturbed medium as

$$\delta X_r(s) = \begin{bmatrix} \delta q_r \\ \\ \delta p_r \end{bmatrix} = \int_{s_0}^{s} \pi_0(s, s')\, \delta B(s')\, ds'$$

where the effective source term, δB, is given by

$$\delta B = \begin{bmatrix} 0 \\ \\ \delta u_q - u^{-1} u_q \delta u \end{bmatrix}$$

where u is the slowness and $u_q = \partial u / \partial q$.

An important aspect of the equations for $\delta X_r(s)$ is that the approximately shifted ray trajectory will not in general hit the receiver. The ray propagator can be used once again to derive an approximate two-point ray,

$$\delta X_{2p} = \begin{bmatrix} \delta q_{\,2p} \\ \\ \delta p_{\,2p} \end{bmatrix}.$$

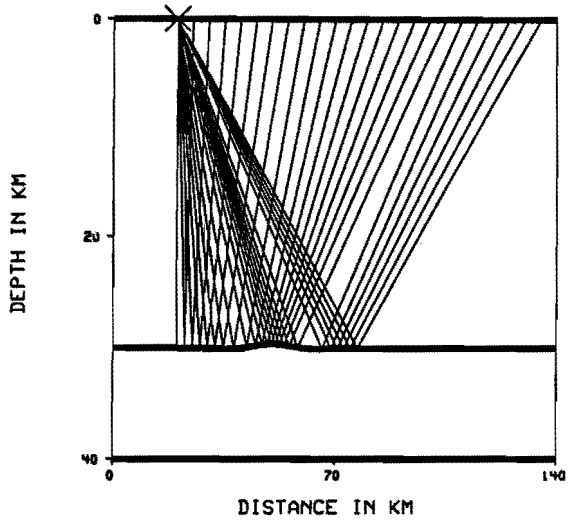

Figure 2: Ray diagram with source at (20., 0.) and 24 rays reflected from a 30 km interface with a .5 km corrugation.

However, this requires an additional approximation for the ray propagator in the perturbed medium.

As an example, the reference ray shift for a direct ray is shown in Figure 1. The model is from 0 to 30 km in depth and -1 to +1 km laterally. The initial unperturbed ray starts at 30 km and goes vertically up to the surface in a homogeneous 6 km/sec medium. A smoothly splined velocity node centered at 15 km depth and -2 km in x is now increased by 2% above the background velocity. The solid line in Figure 1 marked the "perturbed ray" is the exact ray in this new medium with the same initial takeoff angle as the unperturbed ray. This ray bends away from the high velocity node and no longer hits the receiver at (0,0). The dashed line is the approximate perturbed ray. The solid line in Figure 1 marked as the "two-point ray" is the exact ray trajectory from source to receiver. The dot-dash line is the approximate two-point ray by utilizing the unperturbed ray propagator. Note that there is an additional error involved in the two-point perturbed ray than in the perturbed ray.

In order to compare with observed amplitudes, the complete perturbed amplitude must be derived. This includes attenuation, reflection/transmission coefficients, geometric spreading, and receiver functions along the perturbed two-point ray. The approach followed here is to first obtain the approximate two-point ray trajector and then compute the perturbed amplitude directly along this new trajectory.

As an example, a simple test inversion is performed for interface corrugation using travel-time and amplitude. Rays for a single interface corrugation are shown in Figure 2. The initial model has a flat interface and the true model has small interface corrugation. The functional derivatives used in the test inversion are derived using the above travel-time and amplitude perturbations. The travel-time inverted result is shown in Figure 3a and the result using log-amplitude is shown in Figure 3b.

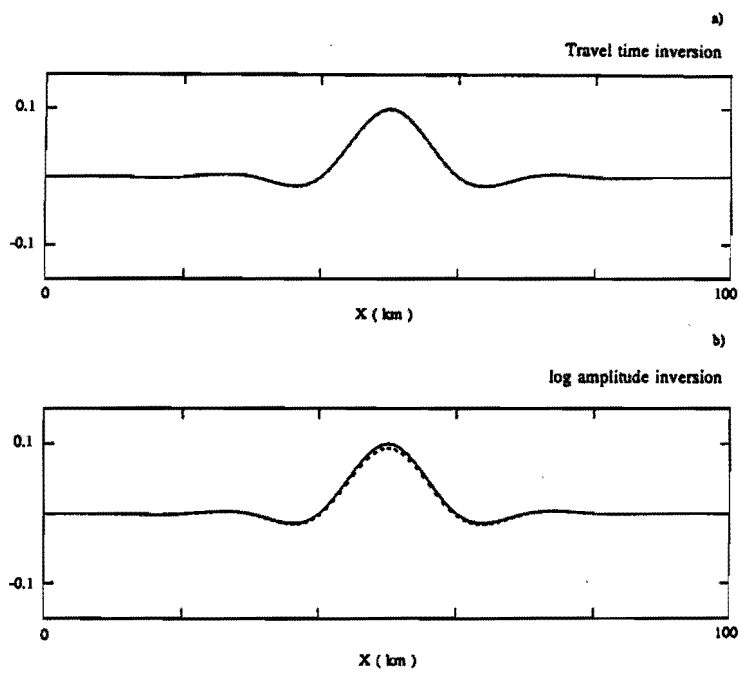

Figure 3: Inversion for 8 splined interface nodes. Exact model has one interface node perturbed by .1 km and is noted by the solid lines.

Work is just beginning in quantifying how large medium variations can be when using perturbation methods for travel-time and amplitude. The existence of singular regions, such as caustics, may also affect the regions of validity for perturbation techniques. For this reason Gaussian beam seismograms, which are a bettef approximation near caustics, may be an important extension when using perturbation methods.

3. Peturbation Methods in Anisotropic Media

Anisotropy can have significant effects on seismic waves and has been detected in the Earth's crust and mantle (Stephen, 1981, Fuchs, 1977). Laboratory measurements imply anisotropy must be widespread in both crystalline and sedimentary rocks (Babuska, 1981; Christensen and Salisbury, 1979). A recent review is given Crampin et. al. (1984).

There are fundamental differences in propagation of seismic waves in isotropic and anisotropic media. In an anisotropic media, the P-wave need not have particle motion normal to the wavefront and propagation velocity is in general different in different directions. In addition, there are two quasi S-waves which can propagate at different velocities giving rise to shear wave splitting as well as polarization anomalies. Phase and group velocities in anisotropic media also diverge resulting

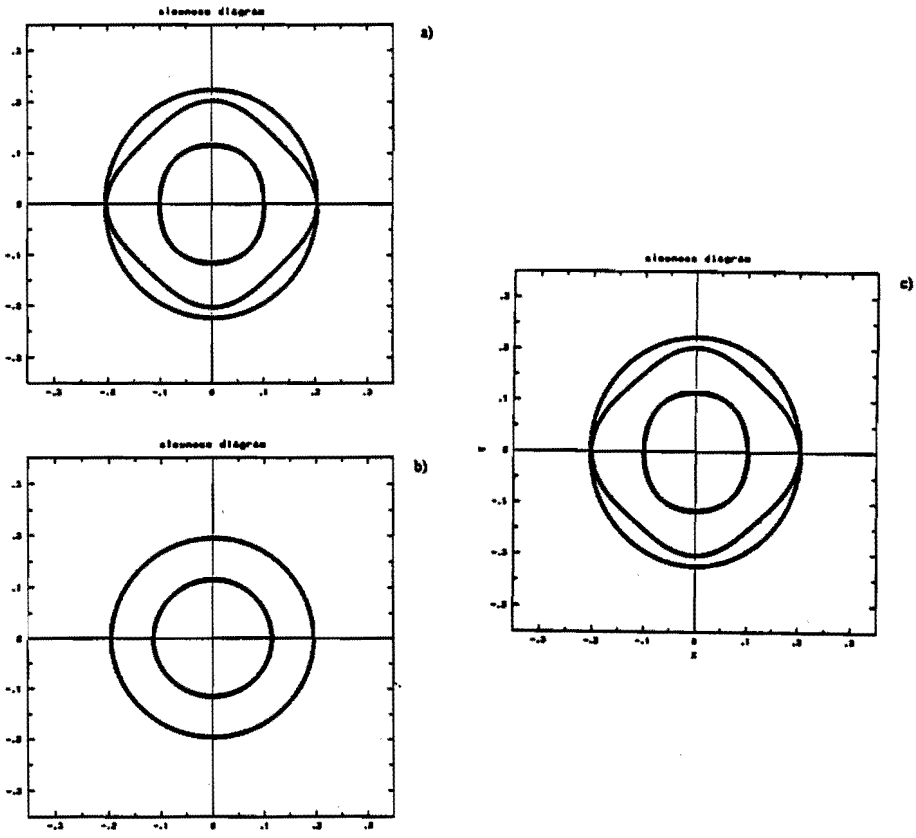

Figure 4: a) Exact anisotropic slowness diagram in the x-z plane. The three branches correspond to the quasi-P and the two quasi-S waves. The units are in sec/km. b) Initial isotropic slowness diagram. c) The slowness diagram found using degenerate perturbation theory from the isotropic case.

potentially in rays that leave the sagittal plane (see Musgrave, 1970; Auld, 1973, Crampin, 1984).

The theory of rays in heterogeneous anisotropic media is well known (see, for example, Červený, 1972), but only recently have complete seismic algorithms been described (see Gajewski and Pšenčík, 1987). The approach for travel-time perturbation theory follows the formulation of Firbas (1984) and Červený and Firbas (1984). An advantage of this approach is that standard isotropic ray algorithms can be used to perform the ray tracing. The perturbation approach is justified for small anisotropy which has most commonly been observed in situ. The elastic parameters are assumed to be of the form

$$a_{ijkl} = c_{ijkl}/\rho = a^0_{ijkl} + a^1_{ijkl}$$

where a^0_{ijkl} are isotropic elastic constants and a^1_{ijkl} are small anisotropic perturbations. If the ray theoretical travel-times have been computed in the nearby isotropic heterogeneous model, the perturbed travel-times in the corresponding anisotropic medium can be approximately found by perturbation.

Recent work by Jech and Pšenčík (1988) has shown that for S-waves, degenerate perturbation theory must be used. This is required to properly separate the combined S-waves in the initial isotropic medium to form two quasi S-waves in the perturbed anisotropic medium. As an example, Figure 4a shows the exact slowness diagram for an orthorhombic material in the x-z plane. The three branches correspond to the quasi P and two quasi S-waves. The units are in sec/km. Figure 4b shows the slowness diagram for a nearby isotropic medium with coalesced S-waves. Figure 4c shows the slowness diagram derived using degenerate perturbation theory (see Nowack and Pšenčík, 1988),. Figure 5 shows the resulting shear wave splitting in travel-times found by perturbation for a linear gradient in a medium with an orthorhombic symmetry. The rays shown below are for a nearby isotropic linear gradient. The approximate shear wave travel-times shown in Figure 5 compare within 5% with travel-times from an exact anisotropic ray calculation.

The calculation of ray theoretical amplitude in a laterally heterogeneous anisotropic media is more difficult. Preliminary results using the perturbation approach have been given by Firbas (1982), but more work on this aspect of the problem is required. In particular, anisotropic dynamic ray equations must be used within amplitude and ray shift perturbation equations. Finally, interfaces need to be incorporated which result in reflected and transmitted anisotropic rays from curved interfaces.

4. Gaussian Beam Seismograms in Perturbed Media

In this section, perturbation of Gaussian beam seismograms to changes in the medium is investigated. The advantage of Gaussian beams over ray theoretical methods is that the results are more complete in singular regions such as caustics and other critical regions (see Červený et al., 1982, Nowack and Aki, 1984, Červený, 1985a, 1985b).

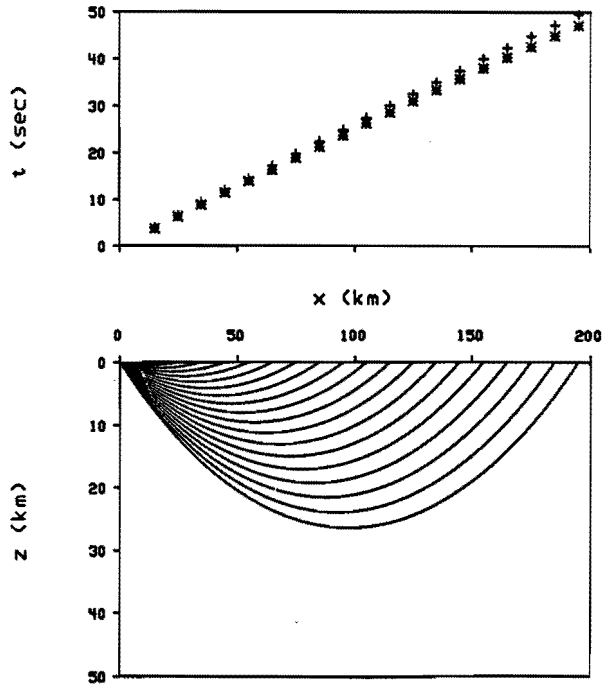

Figure 5: Approximate shear wave splitting found using degenerate perturbation theory for a linear orthorhombic velocity gradient. The rays shown below are for the initial isotropic gradient.

The 2-D Gaussian beam superposition can be written as

$$u(x_r) = \int d\,\gamma\, V(\gamma, x_r, \epsilon)\, e^{i\Theta(\gamma, x_r, \epsilon)} \tag{4.1}$$

where γ is the ray parameter of integration. For a line source in a smoothly heterogeneous medium

$$V(\gamma, x_r, \epsilon) = \frac{i}{4\pi}\left[\frac{\rho(s_0)v(s_0)}{\rho(s)v(s)}\right]^{\frac{1}{2}}\left[\frac{\epsilon}{q_2(s) + \epsilon\, q_1(s)}\right]^{\frac{1}{2}}$$

$$\Theta = \tau(s) + \frac{1}{2}\frac{p_2(s) + \epsilon\, p_1(s)}{q_2(s) + \epsilon\, q_1(s)}\, n^2$$

where $q(s) = q_2(s) + \epsilon\, q_1(s)$ is the complex spreading. (q_1, p_1) and (q_2, p_2) are independent solutions of the ray centered paraxial ray equations (see Červený, 1985a, 1985b), ϵ is a complex free parameter to be specified in order to give bounded beams as well as reduce discretization error (see Klimeš, 1985, 1986). As $\epsilon \to \infty$, a plane wave expansion of the visible spectrum for a line source results. The beam parameter can be equivalently specified at the source or receiver (see Červený, 1985b, Nowack, 1986). If the beam waist is moved to the receiver and in the limit shrunk to zero, the standard ray method results. In terms of a specification at the source this gives

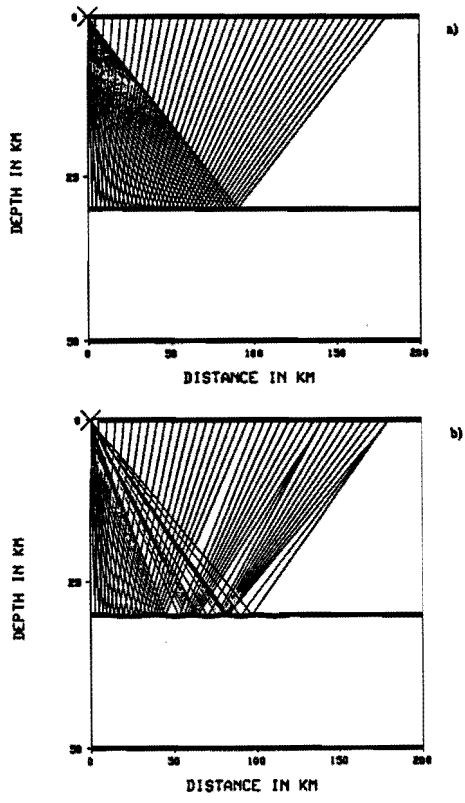

Figure 6: a) Ray diagram for a flat interface. b) Ray diagram for an interface with a .2 km corrugation.

$$\epsilon = -|\frac{q_2}{q_1}| + i\mathrm{Im}\,\epsilon \qquad \mathrm{Im}\,\epsilon < 0$$

This choice avoids coalescence of critical points in the integral expansion (see White et.al., 1987). This is also equivalent to certain beam parameter choices specified at the receiver by Černeý (1985b). The effects of curved interfaces can be included in Eq. (5) by using analogous expressions to Eq. (3) and Eq. (4) (see Černeý, 1985a, 1985b).

Since the Gaussian beam results are made up of individually traced beams in a perturbed medium, each beam can be perturbed independently using results similar to those given in the section on ray perturbations. The individually perturbed beams can then be superposed to give the total perturbed wavefield. The advantage in using Gaussian beams is that two-point ray tracing is not required in either the perturbed or unperturbed case. For the perturbed case, an extra order of approximation in performing the approximate two-point ray tracing is avoided. Also, potential problems in using perturbation theory in the vicinity of caustics are reduced using Gaussian beam theory.

As a preliminary calculation, the reflected wave from a 30 km interface is computed. The ray diagram for a flat Moho is shown in Figure 6a. The 2-D Gaussian beam seismograms are shown in

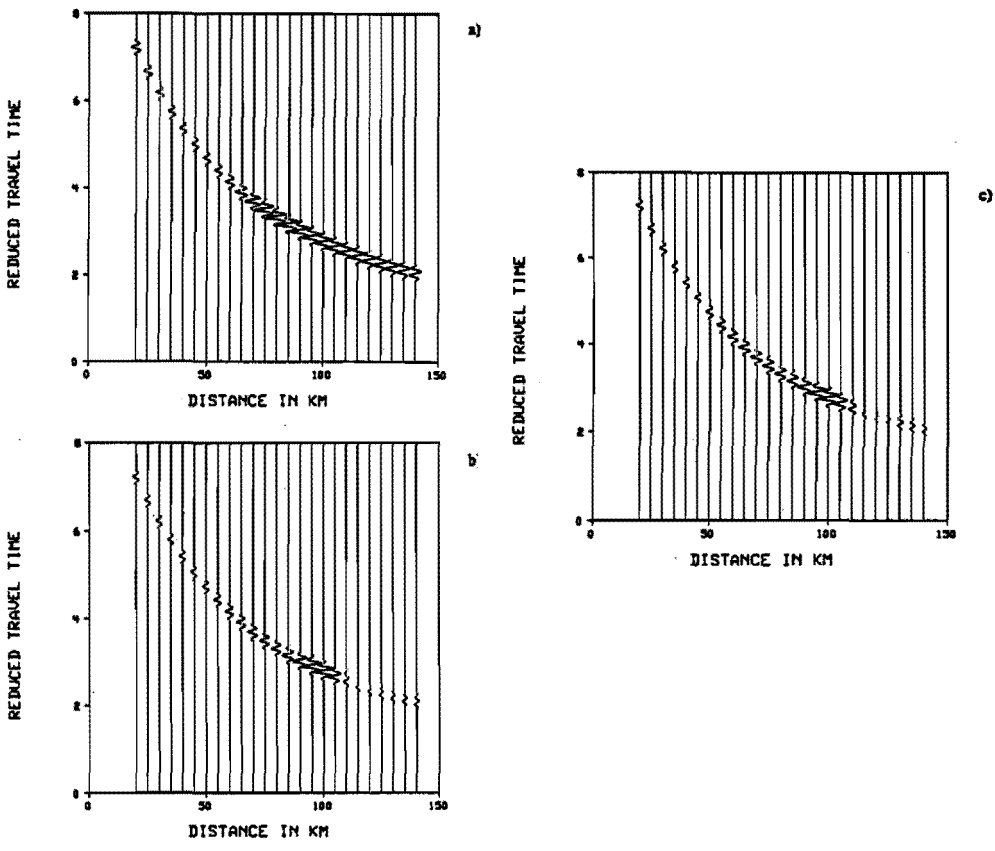

Figure 7: a) Gaussian beam seismograms for a flat interface. b) Gaussian beam seismograms for corrugated interface. c) Approximate Gaussian beams from perturbation theory for corrugated interface.

Figure 7a. The beam parameter, ϵ, has been chosen to suppress the head wave and concentrate on the reflected wave. The critical distance is at 68 km. In Figure 6b, the two-point ray diagram for

a Moho with a .2 km corrugation is shown. The computed Gaussian beam seismograms are shown in Figure 7b. The character of the reflected wavefield has been significantly altered even by this small interface corrugation.

A preliminary perturbation calculation is performed using the unperturbed rays in Figure 6a to approximately compute the reflected wavefield from the Moho corrugation. Each component beam is perturbed and the results are superposed giving the approximate wavefield in Figure 7c. The same beam parameter as for the unperturbed case has been used. The approximate result is seen to be very similar to the direct Gaussian beam calculation using the exact ray trajectories. Further work is required in quantifying the regions of validity of the Gaussian beam perturbation theory, in particular in the vicinity of caustics and critical regions. Perturbed Gaussian beams will have important high-frequency wavefield synthesis applications. In addition, this approach can be used, as in ray theory, to calculate functional derivatives for travel-time, amplitude and waveforms in seismic inversion.

5. Conclusion

Perturbation methods for rays and beams for perturbed heterogeneous media have been discussed in this paper. Perturbation methods are applied to both isotropic and anisotropic media. An important application of perturbation methods is to seismic modeling where simpler nearby models can be used to approximately compute wavefields in more complicated media. This type of analysis is also useful in comparing with more complete seismic synthesis calculations. Further work is still required in constructing higher order perturbation formulations as well as quantifiying regions of validity for the perturbations.

For anisotropic media, perturbation methods have been described which use ray calculations a nearby isotropic medium. For shear waves and shear wave splitting, degenerate perturbation theory is required. The calculation of perturbed amplitudes in anisotropic media still involves extensive developmental work.

An extension to perturbed Gaussian beam seismograms has been implemented. Gaussian beam theory gives more complete results at caustics and other singular regions than ray methods. Gaussian beams have an additional advantage of not using two-point ray tracing, and for perturbed Gaussian beams this requires one less approximation in the perturbation analysis.

References

[1] Aki, K, Christoffersson, A., and Husebye, E.S., "Determination of the three-dimensional seismic structure of the lithosphere, *J. Geophys Res.*, 82, 1977, 277-296.

[2] Auld, B.A., "Acoustic fields and wave in solids, Wiley, New York, 1973.

[3] Babuska, V. "Anisotropy of vp and vs in rock-forming minerals, *J. Geophys* , 50, 1981, 1-6.

[4] Bishop, T.N., Bube, K.P., Butler, R.T., Langan, R.T., Love, P.L., Resnick, J.R., Shuey, R.T., Spindler, D.A. and Wyld, H.W., "Tomographic determination of velocity and depth in laterally varying media," *Geophysics*, 50, 1985, 903-923.

[5] Bording, R.P., Gersztenkorn, A., Lines, L.R., Scales, J.A. and Treitel, S., "Applications of seismic travel-time tomography," *Geophys J.R. astr. Soc.*, 90, 1987, 285-303.

[6] Červený, V. "Seismic rays and ray intensities in inhomogeneous anisotropic media," *Geophys J.R. astr. Soc.*, 29, 1972, 1-13.

[7] Červený, V., "The application of ray tracing to the numerical modeling of seismic wave fields in complex structures, in *'Seismic Exploration'*, Geophysical Press, eds. Treitel, S. and Helbig, K., 15a, 1985a, 1-119.

[8] Červený., V., "Gaussian beam synthetic seismograms," *J. Geophys* , 58, 1985b, 44-72.

[9] Červený, V., and Firbas, P., "Numerical modelling and inversion of travel times of seismic body waves in inhomogeneous anisotropic media," *Geophys J.R. astr. Soc.*, 76, 1984, 41-51.

[10] Červený, V. Popov, M.M. and Pšenčík, "Computation of Wavefields in inhomogeneous Media: Gaussian beam Approach," *Geophys J.R. astr. Soc.*, 70, 1982, 109-128.

[11] Crampin, S., "An introduction to wave propagation in anisotropic media," *Geophys J.R. astr. Soc.*, 76, 1984, 17-28.

[12] Crampin, S., Chesnokov, E.M. and Hipkin, R.G., "Seismic anisotropy - the state of the art: II," *Geophys J.R. astr. Soc.*, 76, 1984, 1-16.

[13] Farra, V. and Madariaga, R., "Seismic waveform modeling in heterogeneous media by ray perturbation theory," *J. Geophys Res.*, 92, 1987, 2697-2712.

[14] Farra, V., Virieux, J. and Madariaga, R., "Ray Perturbation theory for interfaces," *Trans. AGU, EOS*, 69, 1988, 1307.

[15] Firbas, P., "Travel times, amplitudes and synthetic seismograms for slightly anisotropic media," Open File Rep. No. 108, Geophys. Institute University of Karlsruhe, 1982.

[16] Firbas, P., "Travel time curves for complex inhomogeneous slightly anisotropic media," *Studia Geoph. et Geod.*, 28, 1984, 393-406.

[17] Fuchs, K., "Seismic anisotropy of the subcrustal lithosphere as evidence for dynamical process in the upper mantle," *Geophys J.R. astr. Soc.*, 49, 1977, 167-179.

[18] Gajewski, D. and Pšenčík, I., "Computations of high-frequency seismic wavefields in 3-D laterally inhomogeneous anisotropic media," *Geophys J.R. astr. Soc.*, 91, 1987, 383-412.

[19] Jech, J. and Pšenčík, I., "First Order Perturbation Theory for Anisotropic Media", 1988, preprint.

[20] Klimeš, L., "Expansion of a high-frequency time-harmonic wavefield given on an initial surface into Gaussian beams," *Geophys J.R. astr. Soc.*, 79, 1984, 105-118.

[21] Klimeš, L., "Discretization error for the superposition of Gaussian beams, *Geophys J.R. astr. Soc.*, 86, 1986, 531-555.

[22] Musgrave, M.J.P., "Crystal Acoustics,": Holden-Day, San Francisco.

[23] Nowack, R.L. and Aki, K., "The 2-D Gaussian beam method: testing and application, *J. Geophys Res.*, 89, 1984, 7797-7819.

[24] Nowack, R.L., "Gaussian beam synthetic seismograms," *J. of Acoustical Soc. Am.*, 79, 1986, s14.

[25] Nowack, R.L. and Lutter, W.J., "Linearized rays, amplitude, and inversion," *J. Pure and Applied Geophys.*, 128, 1988, 401-421.

[26] Nowack, R.L. and Lyslo, J.A., "Frechet derivatives for curved interfaces in the ray approximation," *Geophysical Journal*, 1989, 97 497-509.

[27] Nowack, R.L. and Pšenčík, I., "Perturbation of Travel Time and Ray Path for Anisotropic Media," Trans. AGU, EOS 69, 1988, p 1329.

[28] Stephen, R.A., "Seismic anisotropy observed in upper oceanic crust," *Geophys. Res. Lett*, 8, 1981, 865-868.

[29] White, B.S., Burridge, R., Noriss, A. and Bayliss, A., "Some remarks on the Gaussian beam summation method," *Geophys J.R. astr. Soc.*, 89, 1987, 579.